Biomimetic Nanocomposite Membranes with Ultrahigh Ion Selectivity for Osmotic Power Conversion

Jianjun Chen,[a,†] Weiwen Xin,[a,b,†] Weipeng Chen[a], Xiaolu Zhao[a], Yongchao Qian[a], Xiang-Yu Kong[a], Lei Jiang[a,b], Liping Wen[a,b,*]

[a]CAS Key Laboratory of Bio-inspired Materials and Interfacial Science, Technical Institute of Physics and Chemistry, Chinese Academy of Sciences, Beijing, 100190, P. R. China
[b]School of Future Technology, University of Chinese Academy of Sciences, Beijing, 100049, P. R. China
[†]These authors contributed equally: Jianjun Chen, Weiwen Xin
[*]Corresponding author: Liping Wen (E-mail: wen@mail.ipc.ac.cn)

Table of the contents:

1. Chemicals and materials

Graphene oxide (thickness 0.8-1.2 nm, diameter 0.5-5 μm) was purchased from J&K Beijing Co., Ltd.; Kevlar yarns were purchased from Dupont; Other chemicals were all analytical grade and purchased from Sigma-Aldrich, USA. Deionized water was prepared by MilliQ system. All reagents were directly used without further purification.

2. Experimental section

Preparation of the aramid nanofiber (ANF) and graphene oxide (GO) dispersion: 1.0 g of bulk Kevlar yarns and 1.5 g of KOH were added into 500 mL of DMSO, and the mixture was stirred for 10 days at room temperature, yielding a dark red ANF dispersion (2 mg/mL). 0.2 mg of GO powder was dispersed and sonicated in 100 ml of DMSO to get a GO dispersion (2 mg/mL).

Fabrication of composite membrane: Initially, a certain amount of ANF solution was added into the GO dispersion, and the mixture was sonicated for 15 min. Then, a desired amount of DI water was added to improve protonation, followed by sonicating for 0.5 h to form a homogeneous suspension. The GO/ANF mixture was vacuum filtered on the nylon filter membrane (47 mm diameter, 0.2 μm pore size) and washed with deionized water for several times. After drying in air, the GO/ANF composite membrane could be peeled off from the nylon filter membrane. The composite membranes were heated at 80℃ for 24 h in the oven to stabilize the membranes.

3. Instruments

SEM images were recorded by a field emission scanning electron microscopy (Hitachi S-4800, Hitachi, Japan) instrument with the acceleration voltage of 5 kV. The morphology images of the ANF and GO were tested by transmission electron microscopy (JEOL, JEM-2100, Japan).

The XRD patterns were collected by a Bruker D8 advance powder diffractometer with Cu Kα radiation (λ = 1.5418 Å) at 40 kV. The mechanical strength of the composite membrane was tested by a forcemeter M5-2 (ESM301, USA) in tensile mode with a tensile speed of 10 mm min^{-1}. Surface zeta potential was tested by the SurPASSTM 3 Zeta Potential Analyzer. The *I-V* measurements and energy tests were performed with a Keithey 6487 semiconductor picoammeter (Keithley Instruments, Cleveland, OH). And the testing membrane area was about 3×10^4 μm^2, the same as previous reports.[1-2]

4. Surface charge calculation

The surface charge density was estimated by Zeta potential test. By using the SurPASSTM 3 Zeta Potential Analyzer, surface zeta potential (ζ) could be obtained. The surface charge density was calculated according to the equation:[3]

$$\sigma_{surface} = \frac{\varepsilon \varepsilon_0 \xi}{\lambda_D}$$

where ε, and ε_0 are the permittivity of water, the permittivity of a vacuum, respectively. And the Debye length (λ_D) can be obtained according equation:[4]

$$\lambda_D = \sqrt{\frac{\varepsilon \varepsilon_0 RT}{2 n_{bulk} z^2 F^2}}$$

where n_{bulk}, and z were the concentration of solution, the valence number, respectively. *F*, *T*, and *R* represented the Faraday's constant, the absolute temperature, and the universal gas constant, respectively.

5. Electrode calibration

In order to explore the osmotic energy harvesting performance, *I-V* tests under a concentration gradient across the membrane were employed. The sweeping voltages from -0.2 V to +0.2 V with a step of 0.02 V was applied. As illustrated in the equivalent circuit of the system, the diffusion potential (E_{diff}) and redox potential (E_{redox}) contribute to the measured V_{OC}. Specifically, E_{diff} is contributed by the power source and E_{redox} is from the unequal potential drop at the electrode-solution interface. Therefore, E_{diff} can be described as:

$$E_{diff} = V_{oc} - E_{redox} \tag{1}$$

Since V_{OC} and E_{redox} can be obtained from the intercept on the voltage axis with and without the composite membrane, respectively, we can obtain the values of E_{diff}. The measured V_{app}, E_{redox} and E_{diff} are shown in Table S1.

6. Energy conversion efficiency

The maximum energy conversion efficiency (η_{max}) can be described as:

$$\eta_{max} = \frac{1}{2}(2t_n - 1)^2 \tag{2}$$

Where t_n is the transfer number of the cation. Since t_n has the maximum value of 1 when the membrane is perfectly cation selective, the energy conversion efficiency has the maximum value of 50%, t_n can be described as:

$$t_n = \frac{1}{2}\left(\frac{E_{diff}}{\frac{RT}{zF}ln(\frac{\gamma_{c_H}c_H}{\gamma_{c_L}c_L})} + 1\right) \tag{3}$$

where E_{diff}, R, T, z, F, γ and c refer to the diffusion potential, universal gas constant, the absolute temperature, charge number, Faraday constant, activity coefficient of ions, ion concentration, respectively.
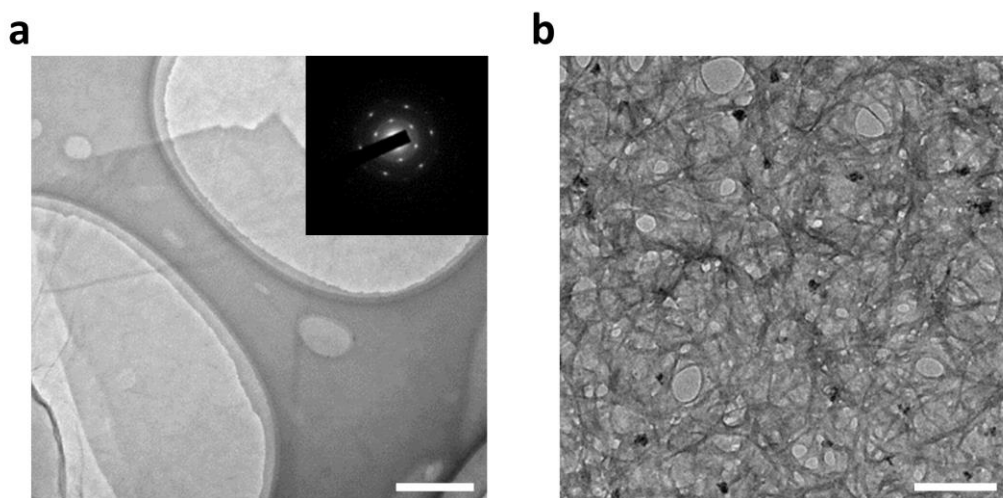
7. Microscopic images.

Figure S1. (a) TEM image of the GO nanosheets. The corresponding SAED pattern and the diffraction spots labeled with Miller-Bravais indices. Scale bar, 0.2 μm. (b) TEM image of the ANF. Scale bar, 0.2 μm. In this process, the use of strong acids and strong oxidizing agents such as H_2SO_4, HNO_3 and $KMnO_4$ could immerse the interlayer of nanosheets and oxidize the sheets with some function groups such as -C-OH, -C-O-C, and -COOH.

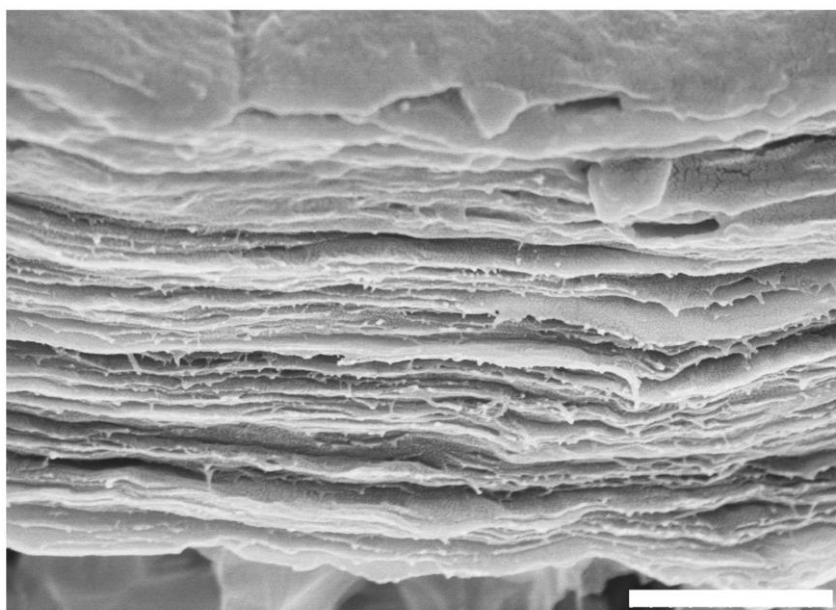
Figure S2. SEM image of the GO/ANF membrane with thickness of ~ 2.2 μm. Scale bar, 1 μm.

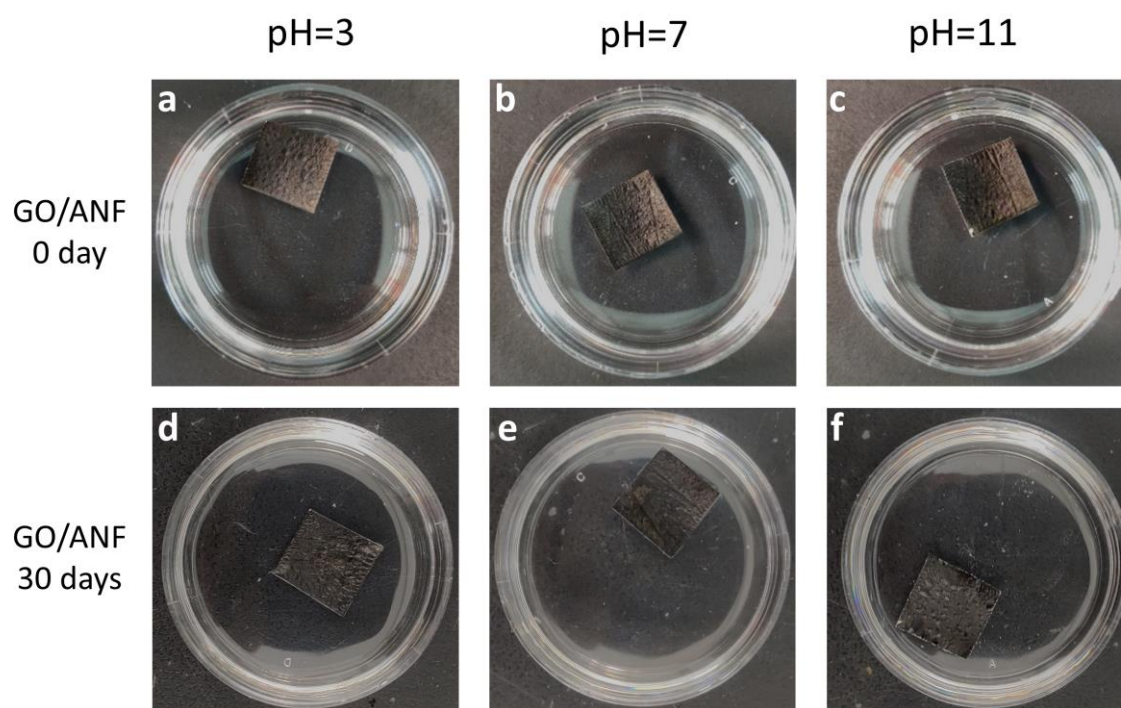## 7. Chemical and physical robustness of the GO/ANF composite membrane.

Figure S3. Stability of the GO/ANF membranes in saline solution. (a, b, c) Photographs of GO/ANF membranes which are just immersing in acidic solution (a), neutral solution (b) and basic solution (c). (d, e, f) Photographs of GO/ANF membranes which have immersed in acidic solution (d), neutral solution (e) and basic solution (f) for a month.
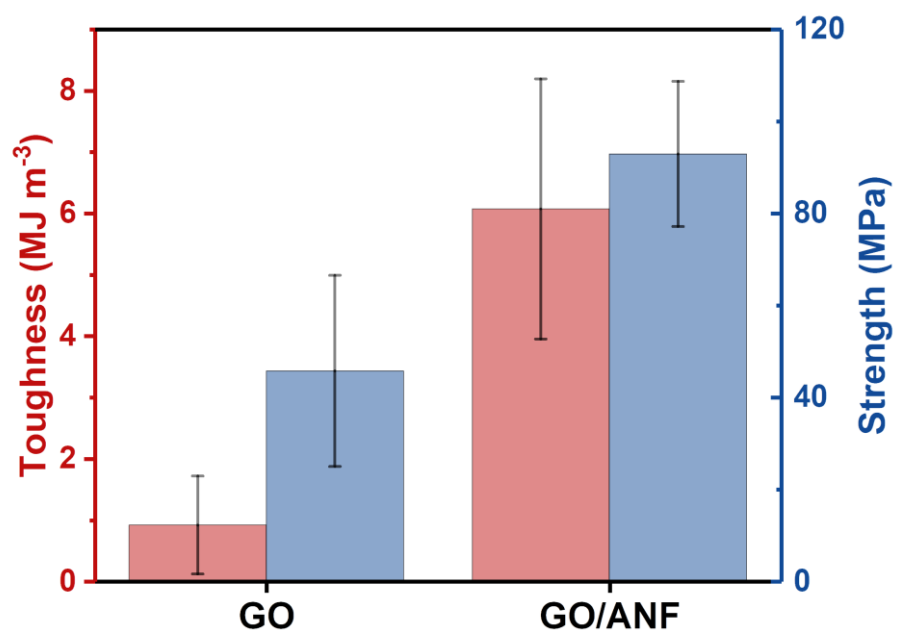
Figure S4. The toughness and tensile strength of the GO and GO/ANF membranes.
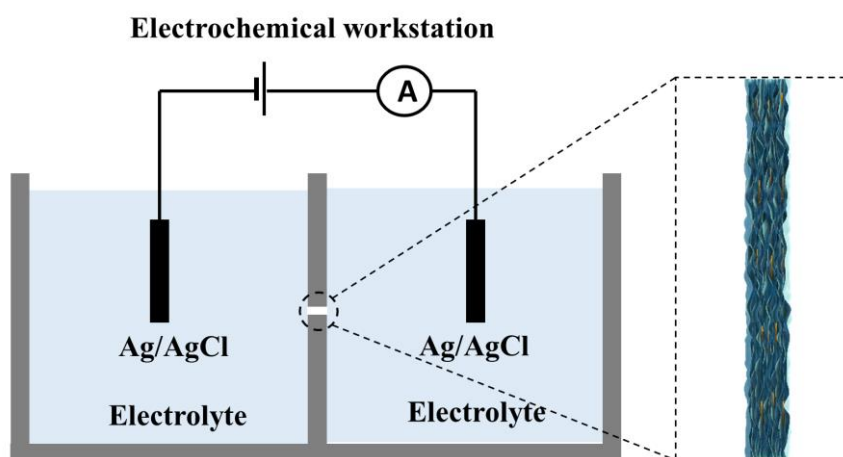
8. Experimental setup

Figure S5. Schematic of the experimental setup.
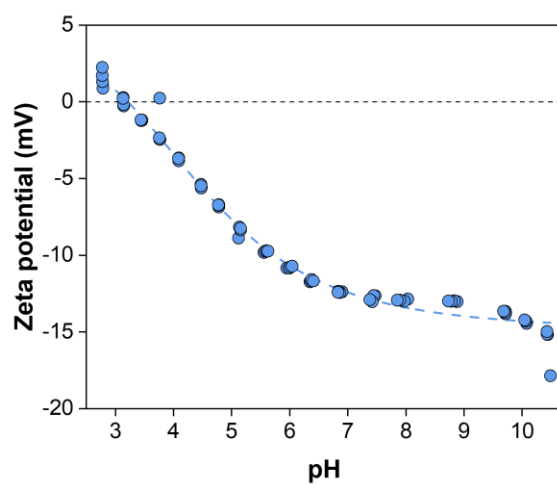
9. Ion transport

Figure S6. The zeta potential of the GO/ANF composite membrane at pH values from 2.77 to 10.44 in 0.01 M KCl.

10. Evaluation of energy conversion
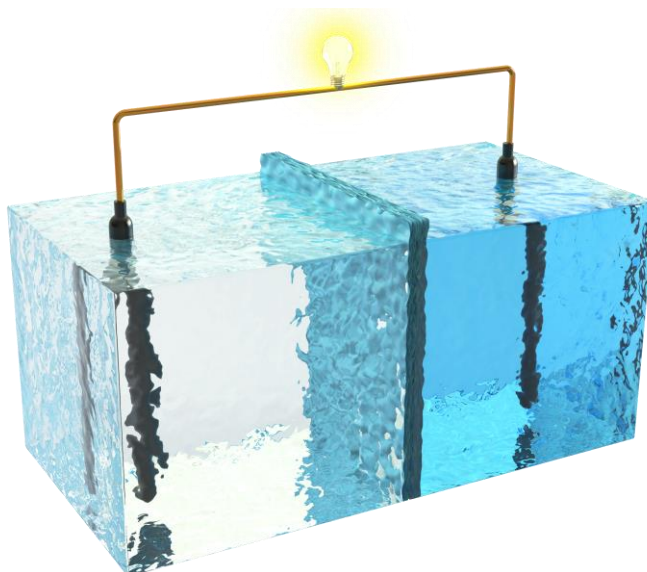
Figure S7. Schematic of the osmotic power converting process under a salinity gradient.

Figure S8. The generated energy conversion efficiency as a function of the salt concentration gradient.

Figure S9. (a) Dependence of the output power density on the electrolyte concentration gradient. C_L was fixed at 0.01 M NaCl. (b) The output power density achieves the maximum values of 0.34, 5.06, and 14.17 W/m^2, respectively, for the 5-fold, 50-fold, and 500-fold salinity gradient.
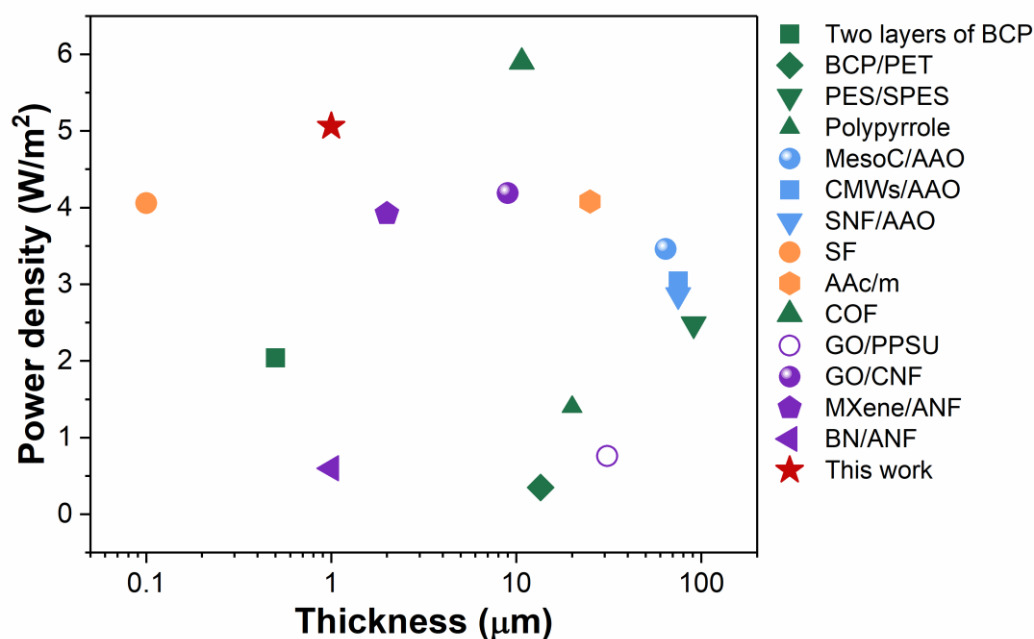
Figure S10. Comparison of energy conversion performance of state-of-the-art osmotic power generators, including two type block copolymer (BCP) hybri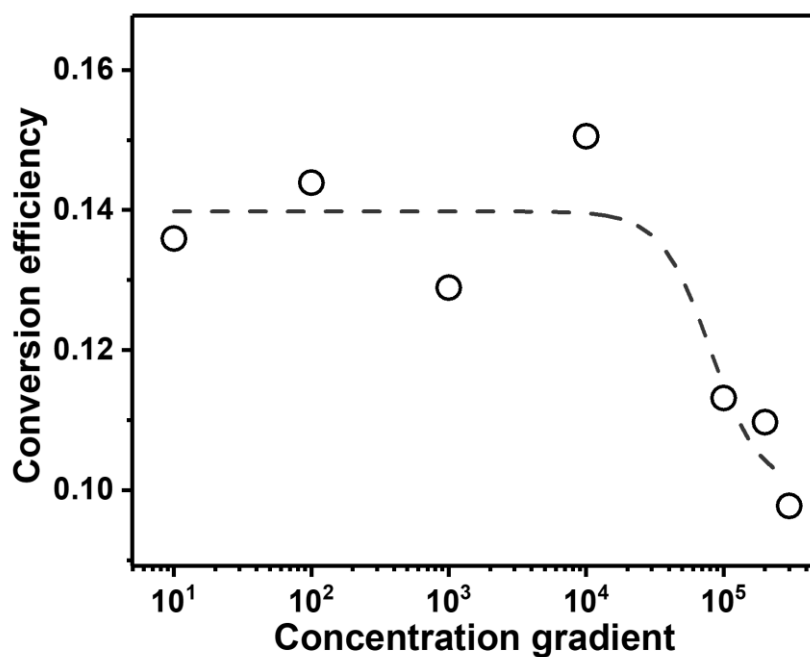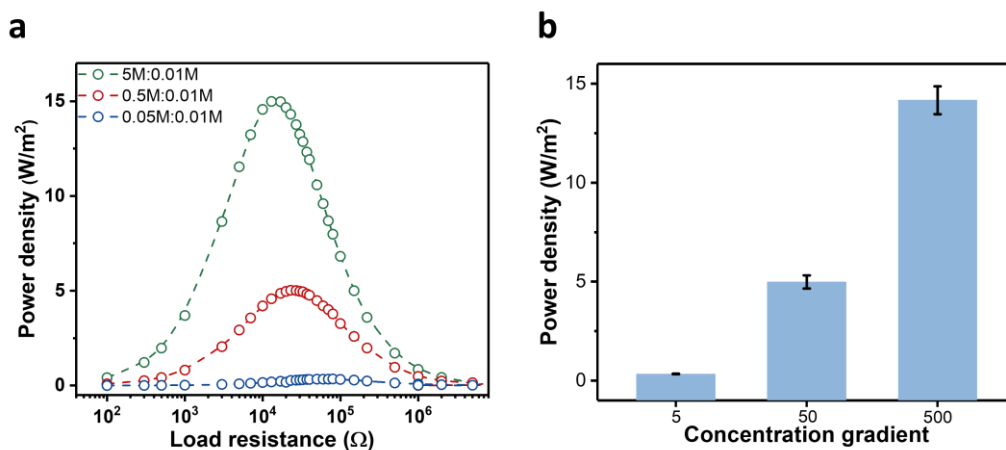d membranes,[5] BCP/polyethylene terephthalate (PET) membranes,[6] polyether sulfone/sulfonated polyether sulfone (PES/SPES) membranes,[7] polypyrrole,[8] mesoporous carbon/macroporous alumina (AAO) hybrid membranes,[9] carbon mesoporous nanowires (CMWs)/AAO membranes,[10] silk nanofiber (SNF)/AAO membranes,[2] silk fibroin (SF) membrane,[11] acrylic acid–co-acrylamide–co-methyl methacrylate (AAc/m) hydrogels,[12] covalent organic frameworks (COF) membrane,[13] graphene oxide/polymer polyphenylsulfone (GO/PPSU) membranes,[14] GO/ cellulose nanofibers (CNF) membrane,[15] MXene/ANF membranes,[1] boron nitride (BN)/ANF membrane,[16] and this work.

Table S1. Comparison of mechanical properties among GO/ANF membranes.[17-21]

No	Methods	ANF content (wt. %)	Tensile strength (MPa)	Tensile modulus (GPa)	Toughness (MJ m^{-3})	Ref.
1		99.75	263±4	12.92±0.27	/	
2		99.5	359±7	19.84±0.23	/	
3		99.25	377±3	18.36±0.87	/	17
4	Vacuum-assisted filtration	99	360±4	10.64±0.73	/	
5		98	236±4	4.88±0.22	/	
6		96	224±4	4.58±0.25	/	
7		99	327.17	/	/	18
8		25	100.6 ± 7.9	13.0 ± 1.4	/	19
9		20	92.89	/	6.069	This work
10	Layer-by-layer assembly	25	/	0.14-0.25	/	20
12		Unknown	688	/	/	21

Table S2. The corresponding values of V_{oc}, E_{redox}, and E_{diff}.

Concentration gradient (M/M)	$10^{-5}/10^{-4}$	$10^{-5}/10^{-3}$	$10^{-5}/10^{-2}$	$10^{-5}/10^{-1}$	$10^{-5}/1$	$10^{-5}/2$	$10^{-5}/3$
V_{oc} (mV)	47.0	105.5	160.4	216.2	236.7	248.6	261.7
E_{redox} (mV)	16.3	43.3	70.7	87.0	96.7	102.3	119.1
E_{diff} (mV)	30.7	62.2	89.7	129.2	140.0	146.3	142.6

(1)   Zhang, Z.; Yang, S.; Zhang, P.; Zhang, J.; Chen, G.; Feng, X., Mechanically strong MXene/Kevlar nanofiber composite membranes as high-performance nanofluidic osmotic power generators. *Nat. Commun.* **2019,** *10*, 2920.

(2)   Xin, W.; Zhang, Z.; Huang, X.; Hu, Y.; Zhou, T.; Zhu, C.; Kong, X.-Y.; Jiang, L.; Wen, L., High-performance silk-based hybrid membranes employed for osmotic energy conversion. *Nat. Commun.* **2019,** *10*, 3876.

(3)   Schaep, J.; Vandecasteele, C., Evaluating the charge of nanofiltration membranes. *J. Membr. Sci.* **2001,** *188*, 129-136.

(4)   Gray, C. G.; Stiles, P. J., Nonlinear electrostatics: the Poisson–Boltzmann equation. *Eur. J. Phys.* **2018,** *39*, 053002.

(5)   Zhang, Z.; Sui, X.; Li, P.; Xie, G.; Kong, X.-Y.; Xiao, K.; Gao, L.; Wen, L.; Jiang, L., Ultrathin and Ion-Selective Janus Membranes for High-Performance Osmotic Energy Conversion. *J. Am. Chem. Soc.* **2017,** *139*, 8905-8914.

(6)   Zhang, Z.; Kong, X.-Y.; Xiao, K.; Liu, Q.; Xie, G.; Li, P.; Ma, J.; Tian, Y.; Wen, L.; Jiang, L., Engineered Asymmetric Heterogeneous Membrane: A Concentration-Gradient-Driven Energy Harvesting Device. *J. Am. Chem. Soc.* **2015,** *137*, 14765-14772.

(7)   Huang, X.; Zhang, Z.; Kong, X.-Y.; Sun, Y.; Zhu, C.; Liu, P.; Pang, J.; Jiang, L.; Wen, L., Engineered PES/SPES nanochannel membrane for salinity gradient power generation. *Nano Energy* **2019,** *59*, 354-362.

(8)   Yu, C.; Zhu, X.; Wang, C.; Zhou, Y.; Jia, X.; Jiang, L.; Liu, X.; Wallace, G. G., A smart cyto-compatible asymmetric polypyrrole membrane for salinity power generation. *Nano Energy* **2018,** *53*, 475-482.

(9)   Gao, J.; Guo, W.; Feng, D.; Wang, H.; Zhao, D.; Jiang, L., High-Performance Ionic Diode Membrane for Salinity Gradient Power Generation. *J. Am. Chem. Soc.* **2014,** *136*, 12265-12272.

(10)   Xie, L.; Zhou, S.; Liu, J.; Qiu, B.; Liu, T.; Liang, Q.; Zheng, X.; Li, B.; Zeng, J.; Yan, M.; He, Y.; Zhang, X.; Zeng, H.; Ma, D.; Chen, P.; Liang, K.; Jiang, L.; Wang, Y.; Zhao, D.; Kong, B., Sequential Superassembly of Nanofiber Arrays to Carbonaceous Ordered Mesoporous Nanowires and Their Heterostructure Membranes for Osmotic Energy Conversion. *J. Am. Chem. Soc.* **2021,** *143*, 6922-6932.

(11)   Chen, J.; Xin, W.; Kong, X.-Y.; Qian, Y.; Zhao, X.; Chen, W.; Sun, Y.; Wu, Y.; Jiang, L.; Wen, L., Ultrathin and Robust Silk Fibroin Membrane for High-Performance Osmotic Energy Conversion. *ACS Energy Lett.* **2020,** *5*, 742-748.

(12)   Chen, W.; Zhang, Q.; Qian, Y.; Xin, W.; Hao, D.; Zhao, X.; Zhu, C.; Kong, X.-Y.; Lu, B.; Jiang, L.; Wen, L., Improved Ion Transport in Hydrogel-Based Nanofluidics for Osmotic Energy Conversion. *ACS Cent. Sci.* **2020,** *6*, 2097-2104.

(13)   Hou, S.; Ji, W.; Chen, J.; Teng, Y.; Wen, L.; Jiang, L., Free-Standing Covalent Organic Framework Membrane for High-Efficiency Salinity Gradient Energy Conversion. *Angew. Chem. Int. Ed.* **2021,** *60*, 9925-9930.

(14)   Zhu, X.; Zhou, Y.; Hao, J.; Bao, B.; Bian, X.; Jiang, X.; Pang, J.; Zhang, H.; Jiang, Z.; Jiang, L., A Charge-Density-Tunable Three/Two-Dimensional Polymer/Graphene Oxide Heterogeneous Nanoporous Membrane for Ion Transport. *ACS Nano* **2017,** *11*, 10816-10824.

(15)   Wu, Y.; Xin, W.; Kong, X.-Y.; Chen, J.; Qian, Y.; Sun, Y.; Zhao, X.; Chen, W.; Jiang, L.; Wen, L., Enhanced ion transport by graphene oxide/cellulose nanofibers assembled membranes for high-performance osmotic energy harvesting. *Mater. Horiz.* **2020,** *7*, 2702-2709.

(16)   Chen, C.; Liu, D.; He, L.; Qin, S.; Wang, J.; Razal, J. M.; Kotov, N. A.; Lei, W., Bio-inspired Nanocomposite Membranes for Osmotic Energy Harvesting. *Joule* **2020,** *4*, 247-261.

(17)   Wang, F.; Wu, Y.; Huang, Y., Novel application of graphene oxide to improve hydrophilicity and mechanical strength of aramid nanofiber hybrid membrane. *Compos. Part A Appl. Sci. Manuf.* **2018,** *110*, 126-132.

(18)   Wu, Y.; Wang, F.; Li, X.; He, J.; Huang, Y., Fabrication of a graphene oxide/nanoscale aramid fiber composite membrane with improved hydrophilicity and mechanical strength via a fast-drying method using absolute ethanol as proton donor. *J. Mater. Sci.* **2018,** *53*, 16383-16392.

(19)   Kwon, S. R.; Harris, J.; Zhou, T.; Loufakis, D.; Boyd, J. G.; Lutkenhaus, J. L., Mechanically Strong Graphene/Aramid Nanofiber Composite Electrodes for Structural Energy and Power. *ACS Nano* **2017,** *11*, 6682-6690.

(20)   Chen, C.; Liu, D.; Qing, X.; Yang, G.; Wang, X.; Lei, W., Robust Membrane for Osmotic Energy Harvesting from Organic Solutions. *ACS Appl. Mater. Interfaces* **2020,** *12*, 52771-52778.

(21)   Chen, C.; Liu, D.; Yang, G.; Wang, J.; Wang, L.; Lei, W., Bioinspired Ultrastrong Nanocomposite Membranes for Salinity Gradient Energy Harvesting from Organic Solutions. *Adv. Energy Mater.* **2020,** *10*, 1904098.